p53 mutant mice that display early ageing-associated phenotypes

Stuart D. Tyner*†, Sundaresan Venkatachalam†‡, Jene Choi‡, Stephen Jones§, Nader Ghebranious‖, Herbert Igelmann¶, Xiongbin Lu‡, Gabrielle Soron‡, Benjamin Cooper‡, Cory Brayton#, Sang Hee Park☆, Timothy Thompson☆, Gerard Karsenty††, Allan Bradley†‡‡‡ & Lawrence A. Donehower‡§§

** Cell and Molecular Biology Program; ‡ Department of Molecular Virology and Microbiology; # Center for Comparative Medicine; ☆ Scott Department of Urology; †† Department of Human and Molecular Genetics; and §§ Department of Molecular and Cellular Biology, Baylor College of Medicine, Houston, Texas 77030, USA*
§ Department of Cell Biology, University of Massachusetts Medical Center, Worcester, Massachusetts 01655, USA
‖ Marshfield Medical Research Foundation, 1000 North Oak Avenue, Marshfield, Wisconsin 54449, USA
¶ Heinrich-Pette-Institut für Experimentelle Virologie und Immunologie an der Universitat Hamburg, Martinistrasse 52, D-20251 Hamburg, Germany
‡‡ The Sanger Centre, Wellcome Trust Genome Campus, Cambridgeshire CB10 1SA, UK
† These authors contributed equally to this work

The p53 tumour suppressor is activated by numerous stressors to induce apoptosis, cell cycle arrest, or senescence. To study the biological effects of altered p53 function, we generated mice with a deletion mutation in the first six exons of the *p53* gene that express a truncated RNA capable of encoding a carboxy-terminal p53 fragment. This mutation confers phenotypes consistent with activated p53 rather than inactivated p53. Mutant ($p53^{+/m}$) mice exhibit enhanced resistance to spontaneous tumours compared with wild-type ($p53^{+/+}$) littermates. As $p53^{+/m}$ mice age, they display an early onset of phenotypes associated with ageing. These include reduced longevity, osteoporosis, generalized organ atrophy and a diminished stress tolerance. A second line of transgenic mice containing a temperature-sensitive mutant allele of p53 also exhibits early ageing phenotypes. These data suggest that p53 has a role in regulating organismal ageing.

The p53 tumour suppressor protein responds to a variety of cellular stresses, including DNA damage, hypoxia and aberrantly activated oncogenes, and may induce cell cycle arrest or apoptosis[1–3]. Studies on cultured primary cells have linked p53 activation to cellular replicative senescence—a terminal cell cycle arrest state reached after a finite number of cell divisions[4]. When cultured human diploid fibroblasts senesce, the activation state of p53 increases[5–7]. Introduction of viral oncoproteins, mutant p53 forms, or anti-p53 antibodies (which inactivate wild-type p53) delay senescence of human primary cells[8–10]. Introduction of oncogenic Ras into primary murine fibroblasts is initially mitogenic, but then induces a premature senescence dependent on wild-type p53 (ref. 11). These data are consistent with hypotheses that cellular replicative senescence serves as a mechanism of tumour suppression[4,12,13].

Recent reports about genetically engineered mice with altered longevity phenotypes implicate p53 as a mediator of organismal senescence[14–18]. Late-generation telomerase-deficient mice exhibit shortened telomeres, decreased longevity and early senescence-related phenotypes[14]. Cells from these mice showed high levels of activated p53 (ref. 15). Crossing of the telomerase-deficient mice with p53-deficient mice resulted in rescue of some senescence-related phenotypes[15]. Early senescence phenotypes were also attributed to a Ku80-deficient mouse that was defective for double-stranded DNA break repair[16]. Embryonic fibroblasts from these mice showed a premature senescence that was rescued by p53 deficiency[17]. $p66^{Shc}$ null mice displayed 30% enhanced longevity compared with wild-type mice[18]. $p66^{Shc}$ mediates a stress response to reactive oxygen species, and cells from the deficient mice exhibited a defective p53 apoptotic response[18].

A direct test of the involvement of p53 in the longevity of organisms could involve modulation of p53 levels in the mouse. We, and others, have generated p53-deficient mice[19–21], but were prevented from studying ageing by early tumours. Conversely, attempts to generate mice that overexpress wild-type p53 have been unsuccessful, probably owing to deleterious effects of increased p53 on the developing embryo (A. Bernstein and J. Butel, personal communication). We report the serendipitous development of a genetically altered mouse that may express a truncated form of p53 that augments wild-type p53 activity. Mice with this defective p53 allele (which we term the 'm' allele) are highly resistant to tumours and display early onset of phenotypes associated with ageing. A second line of transgenic mice containing multiple copies of a temperature-sensitive mutant p53 allele[22] also displayed some of the phenotypes of early ageing observed in $p53^{+/m}$ mice. The observation of such early ageing phenotypes in two distinct p53 mutant lines implicates p53 as a regulator of organismal ageing.

Generation of $p53^{+/m}$ mice

The $p53^{+/m}$ mouse was obtained following an aberrant gene-targeting event in embryonic stem cells. Initially, a p53 targeting construct containing a mutation at codon 245 (Arg245Trp) in p53 was introduced into embryonic stem cells (Fig. 1a). In one embryonic stem cell clone, the 3′ segment of the targeting construct recombined with the endogenous p53 allele. Southern hybridization and polymerase chain reaction (PCR) assays revealed that the modified allele retained p53 exons 7–11 (including the codon 245 mutation) while deleting p53 exons 1–6 and an undefined region upstream of p53 (Fig. 1a, b). Preliminary mapping experiments indicate that the m-allele deletion extends over 20 kilobases (kb) upstream of p53. The deletion extends beyond the nearest *p53* proximal gene, *Efnb3* (S.D.T. and X.L., unpublished data).

We generated mice containing the p53 m allele ($p53^{+/m}$ mice). When the $p53^{+/m}$ mice began to show unexpected phenotypes (see below), we determined that the p53 m allele was expressed as a messenger RNA. Using the 5′ rapid amplification of complementary DNA ends (RACE) procedure, we identified a discrete amplified fragment in tissues of $p53^{+/m}$ mice that was not found in tissues of $p53^{+/+}$ mice. The sequence revealed a chimaeric message containing a 55-bp leader of unknown origin spliced into exon 7 of p53 (Fig. 1c). The foreign leader sequence contained no AUG codons, whereas the p53 exon 7 portion of the message contained three in-frame AUG codons, the third (Met codon 243) being adjacent to a viable translation initiation signal (Fig. 1c). Thus, the chimaeric

m-allele message could produce a C-terminal p53 fragment with a relative molecular mass of roughly 24,000 (M_r 24K). To confirm this, transcripts of the m allele were generated by *in vitro* transcription and then translated by *in vitro* translation. As expected, a protein of 24K was produced that could be immunoprecipitated by a monoclonal antibody specific for the C terminus of p53 (Fig. 1e). However, to date we have been unable to detect the m protein in $p53^{+/m}$ mouse tissues.

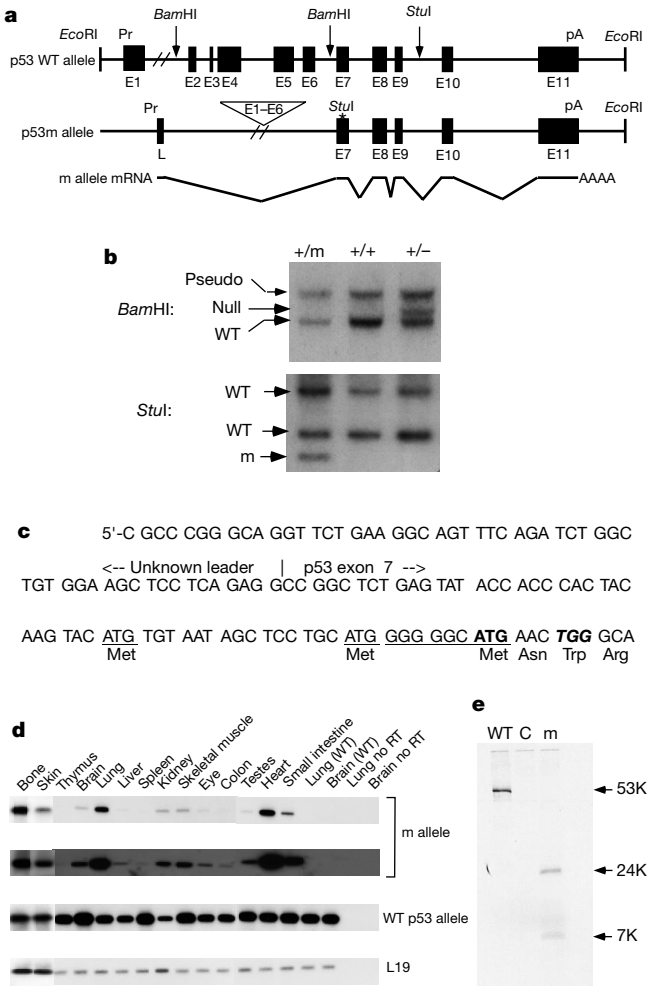

Figure 1 Structure and expression of the mutant p53 m allele. **a**, Maps of the p53 wild-type (WT) and m alleles. Exons 1–6 and upstream sequences are deleted in the p53 m allele, juxtaposing exons 7–11 to an unknown promoter that initiates a chimaeric mRNA containing a 55-nucleotide leader (L) spliced into exons 7–11. Pr, promoter; pA, polyadenylation site. **b**, Southern analysis of tail DNAs from $p53^{+/+}$, $p53^{+/-}$ and $p53^{+/m}$ mice. The top panel shows tail DNAs cleaved with *Bam*HI and hybridized to a p53 exon 2–6 probe to differentiate p53 + and – alleles. The bottom panel shows DNAs cleaved with *Stu*I and hybridized to a p53 exon 5–10 probe to distinguish p53 + and m alleles. **c**, Structure of m-allele mRNA. A 5′ leader of unknown origin is spliced to the 5′ boundary of p53 exon 7. This message contains three in-frame AUG codons. The third AUG codon is a viable translation initiation site (bold and underline), which may produce a C-terminal p53 fragment. The Arg245Trp codon change is indicated (italic and bold). **d**, RT-PCR analysis of tissues of $p53^{+/m}$ and $p53^{+/+}$ mice with primers specific for the m and wild-type p53 alleles. Top and second panel (15× exposure of the top panel) show that most tissues of $p53^{+/m}$ mice express the m-allele RNA, albeit at lower levels than wild-type p53 RNA (third panel). L19 RT-PCR reactions (fourth panel) provide controls. **e**, Protein-coding potential of p53 m-allele RNA. Constructs containing wild-type (WT) p53, no insert (C), or m-allele cDNA were transcribed and translated *in vitro*, and immunoprecipitated with a p53 C-terminal monoclonal antibody. The m-allele construct generated the predicted 24K protein.

To determine the expression pattern of p53 m-allele mRNA *in vivo*, we carried out PCR with reverse transcription (RT-PCR) assays specific for m-allele and wild-type p53 mRNAs. Most tissues of the $p53^{+/m}$ mice, but not the $p53^{+/+}$ mice, expressed m-allele mRNA, but at lower levels than that for wild-type p53 RNA (Fig. 1d).

Enhanced tumour resistance and altered longevity

We monitored the $p53^{+/m}$ mice for the presence of tumours over their lifespan. None of the 35 $p53^{+/m}$ mice developed overt, life-threatening tumours, whereas over 80% of $p53^{+/-}$ mice and over 45% of $p53^{+/+}$ mice developed such tumours (Table 1). On histopathological examination of the $p53^{+/m}$ mice, 2 out of 35 were observed to have localized tumour lesions. One mouse had a focal lung adenoma and another had a well-differentiated bronchioalveolar lung adenocarcinoma (Table 1). In contrast, $p53^{+/+}$ and $p53^{+/-}$ mice developed large tumours of varied type, including lymphomas, osteosarcomas, soft tissue sarcomas and carcinomas.

Given the enhanced tumour resistance in $p53^{+/m}$ mice, it might be expected that their longevity would exceed that of the more tumour-prone $p53^{+/+}$ mice. In fact, the median lifespan of the $p53^{+/m}$ mice was 96 weeks compared with 118 weeks for their $p53^{+/+}$ littermates (Fig. 2a and Table 2). The maximal lifespan of the $p53^{+/m}$ mice was 136 weeks compared with 164 weeks for the $p53^{+/+}$ mice. Statistical comparison of the $p53^{+/m}$ and $p53^{+/+}$ survival curves indicated that the differences in longevity were highly significant ($P < 0.0001$). Histopathological examination of the $p53^{+/m}$ mice failed to reveal any obvious disease-associated phenotypes. A precise cause of death was difficult to determine in many cases. No inflammation or other indicators of infectious diseases above levels seen in $p53^{+/+}$ mice were noted, although subtle differences in immune status or function cannot be ruled out.

To determine whether the altered longevity and tumour resistance in the $p53^{+/m}$ mice were dependent on the presence of wild-type p53, we crossed $p53^{+/m}$ mice to $p53^{-/-}$ mice and obtained $p53^{-/m}$ offspring. If the m-allele product augments the activity of wild-type p53 to enhance tumour resistance, then the absence of wild-type p53 in the $p53^{-/m}$ mice should result in little or no tumour suppression effect when the survival curves of $p53^{-/m}$ and $p53^{-/-}$ mice are compared. Although there is a slight delay in mean tumorigenesis in $p53^{-/m}$ mice compared with $p53^{-/-}$ mice, maximal lifespans of the two genotypes are similar (9–10 months) (Fig. 2b). The tumour types observed in the $p53^{-/m}$ mice were similar to those of the $p53^{-/-}$ mice—primarily T-cell lymphomas and soft tissue sarcomas. Thus, the enhanced tumour resistance conferred by the m allele is dependent on the presence of wild-type p53.

Augmented p53 responses in $p53^{+/m}$ mice

To assess mechanisms of tumour resistance in $p53^{+/m}$ mice, we examined cells and tissues from $p53^{+/m}$, $p53^{+/+}$, $p53^{+/-}$, $p53^{-/m}$ and $p53^{-/-}$ mice for p53-regulated activities. We compared $p53^{+/+}$ and $p53^{+/m}$ mouse embryonic fibroblasts (MEFs) for susceptibility to transformation after infection with an activated *ras* plus *myc* transforming retrovirus. We found that $p53^{+/m}$ MEFs were consistently 2–4-fold more resistant to transformation than their $p53^{+/+}$

Table 1 Tumour types arising in $p53^{+/-}$, $p53^{+/+}$, $p53^{+/m}$ and pL53 mice

Tumour type	$p53^{+/-}$ (n = 217)	$p53^{+/+}$ (n = 56)	$p53^{+/m}$ (n = 35)	pL53 (n = 66)
Lymphoma	49 (28%)	18 (67%)	0	9 (56%)
Osteosarcoma	61 (34%)	2 (7%)	0	0
Soft tissue sarcoma	47 (27%)	3 (11%)	0	1 (6%)
Carcinoma	20 (11%)	4 (15%)	1 (50%)*	5 (31%)*
Other	0	0	1 (50%)†	1 (6%)
Total	177	27	2	16

Values in parentheses indicate the percentage of total tumours.
* Lung adenocarcinoma.
† Small focal lung adenoma.

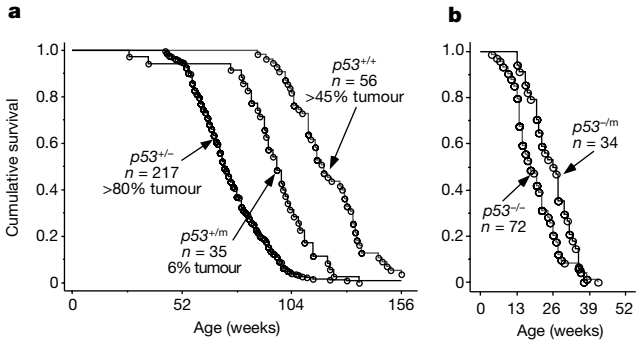

Figure 2 Longevity in $p53^{+/+}$, $p53^{+/-}$, $p53^{+/m}$, $p53^{-/-}$ and $p53^{-/m}$ mice. **a**, Survival of $p53^{+/-}$, $p53^{+/+}$ and $p53^{+/m}$ mice. More than half of the tumours in wild-type mice appeared while many of the $p53^{+/m}$ mice were still alive. **b**, Survival of $p53^{-/-}$ and $p53^{-/m}$ mice. Virtually all of the $p53^{-/-}$ and $p53^{-/m}$ mice developed cancer.

counterparts (Fig. 3a). We also compared transformation efficiencies of $p53^{-/-}$ and $p53^{-/m}$ MEFs. $p53^{-/m}$ cells displayed equivalent susceptibility to transformation as $p53^{-/-}$ cells (Fig. 3a), indicating that transformation resistance mediated by the m allele is dependent on wild-type p53.

After DNA damage, levels of p53 protein increase and p53 activates a number of transcriptional targets, including the $p21^{Waf1/Cip1}$ cyclin-dependent kinase inhibitor. We compared p53 protein stability in kidneys of $p53^{+/+}$, $p53^{+/m}$ and $p53^{+/-}$ mice treated with 5 Gy of ionizing radiation. Before irradiation, p53 protein levels were low, but p53 levels after normalization to an actin control showed a robust increase at 4 h after irradiation for kidney cells of $p53^{+/+}$, $p53^{+/-}$ and $p53^{+/m}$ mice (Fig. 3b). However, by 24 h after irradiation, p53 protein levels in the cells from $p53^{+/-}$ mice were decreased from those observed in $p53^{+/+}$ and $p53^{+/m}$ mice (Fig. 3b). These results indicate that the presence of the m allele may augment p53 protein stability.

$p21^{Waf1/Cip1}$ RNA was compared in MEFs of $p53^{+/+}$, $p53^{+/-}$ and $p53^{+/m}$ mice before and after treatment with 5 Gy of ionizing radiation (Fig. 3c). Before irradiation, MEFs of $p53^{+/+}$ and $p53^{+/m}$ mice exhibited higher levels of basal p21 expression compared with MEFs of $p53^{+/-}$ mice. At 4 h after ionizing radiation treatment, p21 mRNA levels were highest in MEFs of $p53^{+/+}$ mice, with intermediate levels in MEFs of $p53^{+/m}$ mice and relatively lower levels in MEFs of $p53^{+/-}$ mice. By 48 h, levels of p21 remained high in cells of $p53^{+/+}$ and $p53^{+/m}$ mice, but declined in cells of $p53^{+/-}$ mice.

The robust p21 expression in cells of $p53^{+/m}$ mice was corroborated by transfection assays. Saos-2 human osteosarcoma cells (null for p53) were co-transfected with a p21 promoter luciferase reporter construct and various combinations of m, wild-type p53, or empty vector expression constructs. Cells transfected with wild-type p53 or wild-type p53 plus empty vector constructs exhibited more than a tenfold increase in luciferase activity compared with cells transfected with empty vector or m expression constructs alone (Fig. 3d). In four independent experiments, wild-type p53 plus m-allele expression constructs induced a mean 2.3-fold increase in luciferase activity compared with cells transfected with wild-type p53 alone. Moreover, when the amount of the m expression construct was only one-tenth that of the co-transfected wild-type p53 construct, luciferase activity was still significantly higher (1.6-fold) than that produced by wild-type p53 alone. These data indicate that m-allele product can enhance p53 stability and transactivation activity.

Early senescence-associated phenotypes in $p53^{+/m}$ mice

We examined the possibility that the shortened lifespans of $p53^{+/m}$ mice could be accompanied by signs of early ageing. Up to 12 months of age $p53^{+/m}$ mice appear morphologically identical to their $p53^{+/+}$ littermates. However, by 18 months, virtually all of the $p53^{+/m}$ mice exhibit signs of weight loss, lordokyphosis (hunchbacked spine) and an absence of vigour (Fig. 4a–d). Weighing the mice confirmed significant reductions in the body mass of $p53^{+/m}$ mice at 18 and 24 months of age compared with their age-matched $p53^{+/+}$ counterparts (Fig. 4d). In contrast, reduced body weights in the $p53^{+/+}$ mice were not observed until extreme old age (30–36 months) (Fig. 4d). The weight losses of $p53^{+/m}$ mice were not a result of reduced food intake. Young and old $p53^{+/m}$ and $p53^{+/+}$ animals consumed similar amounts of food. Moreover, histological examination of intestinal sections revealed no abnormalities consistent with a reduced ability to absorb nutrients. Blood chemistries of the older $p53^{+/m}$ animals did not reveal any signs of nutritional deficiencies (S.T. and C.B., unpublished data; and data not shown).

Visual, pathological and histopathological examination of young (3 months) $p53^{+/m}$ and $p53^{+/+}$ mice failed to reveal any obvious differences between the two genotypes; however, assessment of old (24 months) $p53^{+/m}$ and $p53^{+/+}$ mice revealed marked differences. Skinned, older $p53^{+/m}$ mice exhibit clear reductions in body mass, adipose tissue deposition, muscle mass and a pronounced lordokyphosis (Fig. 4c). The apparent differences in muscle mass were confirmed by weighing isolated quadriceps femoris muscles from 22–24-month-old $p53^{+/m}$ and $p53^{+/+}$ mice. The mean mass of the quadriceps of male $p53^{+/+}$ mice was almost 2.5-fold that of the quadriceps of male $p53^{+/m}$ mice (data not shown). Spleen, liver, kidney and testes, although not brain, were reduced in mass in $p53^{+/m}$ mice (Fig. 4d–g). The reduced organ masses of $p53^{+/m}$ mice are due to a decrease in overall cellularity. This is demonstrated in

Table 2 Ageing-related phenotypes in $p53^{+/+}$, $p53^{+/m}$ and pL53 mice

Phenotype	$p53^{+/+}$	$p53^{+/m}$	pL53
Median lifespan	118 weeks	96 weeks	ND
Maximum lifespan	164 weeks	136 weeks	ND
Cancer incidence	>45%	<6%	20% (18 months)
Body weight	Reduced at 30 months	Reduced at 18 months	Slightly reduced
Liver, spleen, kidney mass	Minimal loss of mass	25–40% reduced at 24 months	Minimal loss
Lymphoid atrophy	Moderate	Pronounced	Moderate
Lordokyphosis	Modest	Pronounced	Pronounced
Osteoporosis	Minimal	Pronounced	Pronounced
Blood chemistry	Normal	Normal	Normal
Urinalysis	Normal	Normal	ND
Peripheral WBC, RBC	Normal	Normal	Normal
Hair-greying and alopecia	Minimal	Minimal	Some alopecia
Hair regrowth	Modestly reduced	Greatly reduced	Greatly reduced
Dermal thickness	Moderately reduced	Greatly reduced	Moderately reduced
Subcutaneous adipose	Moderately reduced	Greatly reduced	Greatly reduced
Wound-healing	Normal	Retarded	Retarded
Muscle atrophy	Minimal	Pronounced	Minimal
Anaesthetic stress tolerance	Well tolerated	Poorly tolerated	Poorly tolerated
5-FU myeloablation	Robust WBC replenishment	Reduced WBC replenishment	ND

Phenotypes of $p53^{+/+}$ and $p53^{+/m}$ mice were assessed at 24 months of age; phenotypes of pL53 mice were assessed at 16–20 months of age. ND, not done; WBC, white blood cell; RBC, red blood cell.

the spleen sections, where the T- and B-cell-containing white pulp regions in 24-month-old $p53^{+/m}$ mice are markedly reduced in area and cell number compared with those in the spleens of age-matched $p53^{+/+}$ mice (Fig. 4h, i), indicative of a pronounced lymphoid atrophy. Both males and females showed comparable reductions in body weight and organ masses. These results correlate with human ageing, where after the age of 60, reductions in total body, liver, spleen and kidney masses are observed[23].

The pronounced lordokyphosis in old $p53^{+/m}$ mice suggested osteoporosis, an age-related marker in humans and mice[24,25]. X-ray analysis of 3-month-old mice failed to reveal any obvious differences in bone structure or density. By 12 months of age, some of the

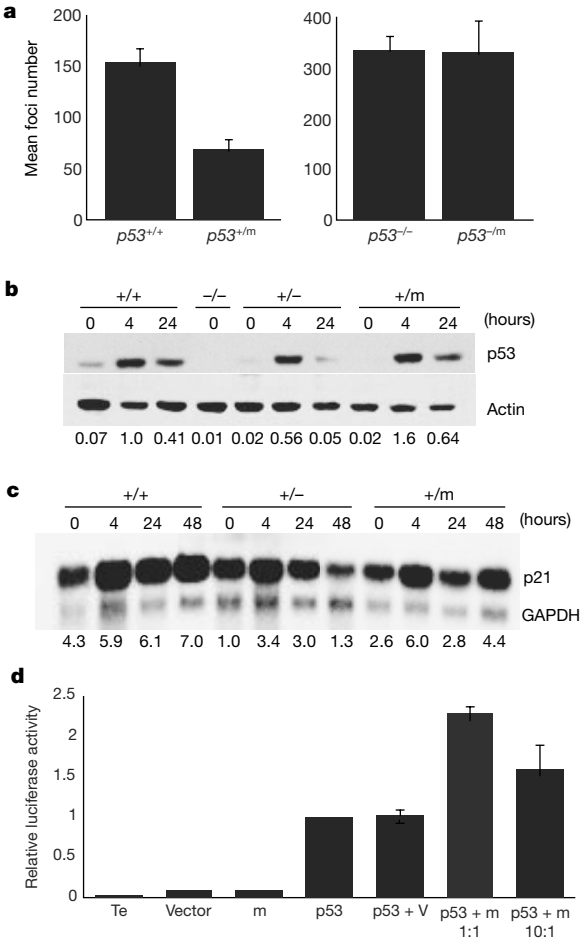

Figure 3 Transformation and p53 response phenotypes. **a**, Transformation susceptibility of $p53^{+/+}$, $p53^{+/m}$, $p53^{-/-}$ and $p53^{-/m}$ embryonic fibroblasts. Left, Comparison of total foci produced by *ras* plus *myc* retroviral infection of 4 plates each of $p53^{+/m}$ and $p53^{+/+}$ MEFs. Right, comparison of total foci produced by *ras* plus *myc* retroviral infection of $p53^{-/-}$ and $p53^{-/m}$ MEFs. **b**, Analysis of p53 protein in kidney cells of $p53^{+/+}$, $p53^{+/m}$ and $p53^{+/-}$ mice before and after treatment with 5 Gy of ionizing radiation. The top panel shows p53 levels detected with an antibody to p53; the lower panel displays actin levels. Values below each lane indicate relative p53 levels after normalization to actin. **c**, Northern blot hybridization showing expression of $p21^{Waf1/Cip1}$ mRNA in MEFs of $p53^{+/+}$, $p53^{+/m}$ and $p53^{+/-}$ mice before and after 5 Gy of ionizing radiation. The upper band is the p21 mRNA signal; the lower band contains the GAPDH signal. Values below each lane indicate relative p21 mRNA levels after normalization to GAPDH levels. **d**, Enhancement of wild-type p53 transactivation activity by the m allele. Saos-2 cell co-transfection assays were performed with a p21 promoter-driven luciferase construct and various combinations of wild-type p53, m allele, or empty vector expression constructs. Relative luciferase activity was normalized to a value of 1.0 produced by wild-type p53 alone. 1:1 and 10:1 refer to the ratio (in μg) of wild-type p53 to m-allele expression construct for each co-transfection. Te, mock transfected cells; V, empty vector.

$p53^{+/m}$ mice began to show global reductions in bone density, which became severe in the 24-month-old $p53^{+/m}$ mice in comparison with age-matched $p53^{+/+}$ littermates (Fig. 5a). The tail, vertebrae, limbs and craniums of the 24-month-old $p53^{+/m}$ mice showed significant reductions in bone density. Histological analysis of cross-sections from 24-month-old $p53^{+/m}$ and $p53^{+/+}$ mice showed reduction in cortical and trabecular bone area compared with tibias of old $p53^{+/+}$ mice (Fig. 5b, c).

Two markers for aged skin in humans are reduced dermal thickness and subcutaneous adipose[26]. Histological cross-sections of dorsal skin revealed no differences in the skin structure of 3-month-old mice, but significant differences were seen in the skin of 24-month-old mice (Fig. 6a–d). Skin of $p53^{+/m}$ mice showed significant reductions in mean dermal thickness compared with skin of $p53^{+/+}$ mice at 24 months (Fig. 6c–e). Although skin of young $p53^{+/m}$ and $p53^{+/+}$ mice had many subcutaneous adipose cells, these cells were virtually absent in skin of old $p53^{+/m}$ mice and reduced in skin of old $p53^{+/+}$ mice (Fig. 6c, d, f).

The hair on the older $p53^{+/m}$ mice appeared to be sparser than that of their $p53^{+/+}$ counterparts. Hair sparseness could be a function of the ratio of hair follicle cells in the anagen (growth) phase to those in the telogen (resting) phase. Using a hair-growth assay—which involves shaving a dorsal segment of skin on the mouse and measuring the amount of hair growth after 20–25 days—hair growth declines linearly as a function of age in mice[27]. Only a modest reduction in hair growth was observed in the young $p53^{+/m}$ mice compared with young $p53^{+/+}$ mice (Fig. 6h). In 22–26-month-old $p53^{+/m}$ mice, almost no hair growth was observed, whereas old $p53^{+/+}$ mice displayed robust hair growth (Fig. 6g, h).

A reduced ability to tolerate stresses is a hallmark of ageing[28]. One such age-related stress, wound healing, is delayed as a function of age in both mice and humans[14,29]. To test this capacity, we placed two 3-mm punch biopsies in the dorsal skin of young and old anaesthetized $p53^{+/m}$ and $p53^{+/+}$ mice. However, we found that many of the old $p53^{+/m}$ mice died after injection with the standard dosage of the anaesthetic Avertin, and a greatly reduced dose had to be used for this age/genotype category. This observation agrees with reports that aged organisms are less able to tolerate the stress of anaesthesia than are younger organisms[30,31].

After adjustment of anaesthetic doses, wounds were induced and monitored over a period of 4 days for closure before sacrifice. Wound diameters at 2, 3 and 4 days after wounding were similar for wounds of young $p53^{+/m}$ and $p53^{+/+}$ mice (Fig. 7a); however, old $p53^{+/m}$ mice exhibited a significant delay in wound closure (Fig. 7b). When cross-sections of the wound at 4 days after wounding were examined by histopathology, there was a frequent reduction in re-epithelialization from the wound edge in the old $p53^{+/m}$ wound compared with that in the wounds of old $p53^{+/+}$ mice (Fig. 6c, d).

An acute stress that measures the response to haematopoietic precursor cell ablation is treatment with 5-fluorouracil (5-FU)[32]. In this assay, we found that young $p53^{+/+}$ and $p53^{+/m}$ mice showed reduced white blood cell counts at day 6 after 5-FU injection, but had recovered by day 11 (Fig. 7e). The old $p53^{+/+}$ mice were not overtly affected by 5-FU treatment, and their white blood cell counts had recovered by day 11. However, the $p53^{+/m}$ mice displayed a marked morbidity after treatment, and one out of six of the old $p53^{+/m}$ mice injected with 5-FU died. Although old $p53^{+/+}$ and $p53^{+/m}$ mice showed similar reductions in white blood cell counts at 6 days after 5-FU injection, the recovery at day 11 was significantly more robust for $p53^{+/+}$ mice than for $p53^{+/m}$ mice ($P = 0.02$) (Fig. 7f).

Although a number of age-associated phenotypes appeared earlier in the $p53^{+/m}$ mice than in the wild-type mice, other age-related changes were not noted. Examination of lungs, heart, brain and intestines failed to reveal any clear differences in the old $p53^{+/+}$ and $p53^{+/m}$ mice. Ageing phenotypes observed in other models, such as liver pathologies[20], hair greying and alopecia[18], atrophy of intestinal villi[18], skin ulceration[18,33], amyloid deposits[33], brain atrophy[33], joint

diseases[33], or cataracts[33] were not increased in frequency in the older $p53^{+/m}$ mice. Blood chemistry, blood cell counts and male fecundity in the older $p53^{+/m}$ mice did not differ from that of older $p53^{+/+}$ mice (Table 2). Thus, the older $p53^{+/m}$ mice display an early onset of some, but not all, phenotypes associated with ageing.

pL53 mice exhibit early ageing-related phenotypes

During our observations on the ageing $p53^{+/m}$ mice, we monitored a colony of mutant p53 transgenic (pL53) mice containing roughly 20 copies of a mutation at codon 135 (Ala135Val), which has been described previously[22]. The protein produced by this mutant allele of p53 is temperature sensitive, and assumes a wild-type conformation at 32.5 °C and a mutant conformation at 37.5 °C (ref. 34). This mutant p53 transgenic mouse is modestly susceptible to a broad array of tumour types, with a 20% tumour incidence by 18 months of age (Table 1)[22]. However, most of the pL53 transgenic mice remain tumour free at 18 months, yet exhibit a generalized lack of robustness compared with their non-transgenic littermates (Fig. 8a, b). Some phenotypes exhibited by the pL53 transgenic mice were similar to those of the older $p53^{+/m}$ mice. For example, by 18–20 months, many of the pL53 mice exhibited sparse, ruffled fur, loss of weight, lordokyphosis and lethargy. Necropsies of these mice usually failed to reveal any overt or microscopic tumours or other pathologies. However, X-rays of representative 18-month-old animals showed evidence of increased osteoporosis in pL53 transgenic mice (Fig. 8c). The ability of the pL53 transgenic mice to regrow hair was also markedly diminished in comparison with matched non-transgenic littermates (Fig. 8d). Moreover, cross-sectional analysis of skin indicated that the transgenic mice had significantly reduced subcutaneous adipose tissue compared with their age- and sex-matched normal littermates (P = 0.001) (Fig. 8e). Finally, the wound-healing assay showed a significant reduction in wound closure for the pL53 transgenic mice 4 days after induction of a 3-mm punch biopsy in the dorsal skin (P = 0.05) (Fig. 8f). Although body weight was often reduced in the 18-month-old pL53 transgenic mice in comparison with similarly aged non-transgenic mice, organ weights (spleen, kidney, liver, testes, skeletal muscle) were only modestly affected. Thus, the older

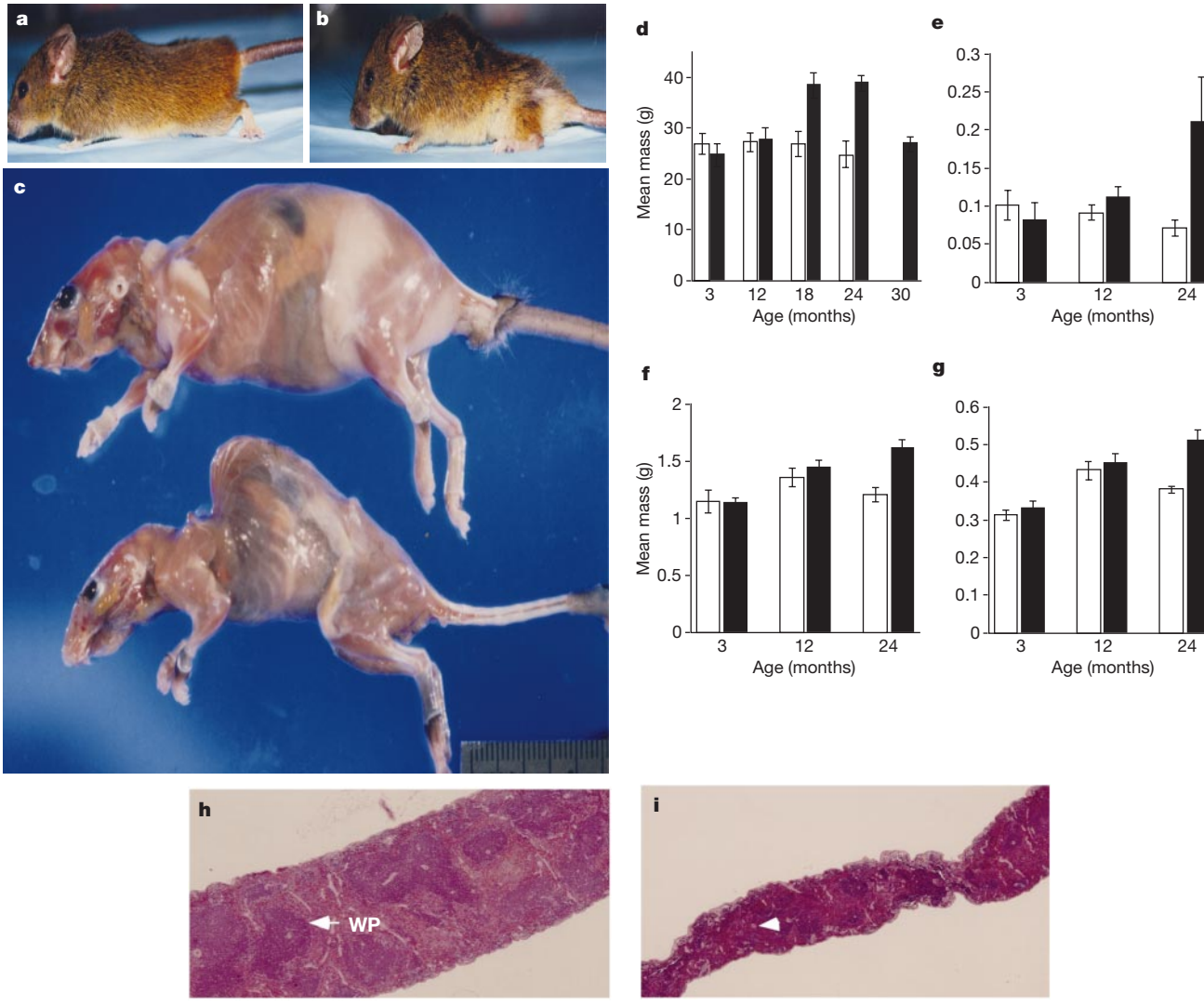

Figure 4 Phenotypes of aged $p53^{+/+}$ and $p53^{+/m}$ mice. **a**, Photograph of a 24-month-old $p53^{+/+}$ male mouse. **b**, Photograph of a 24-month-old $p53^{+/m}$ male mouse showing reduced size and lordokyphosis. **c**, Representative 20-month-old skinned $p53^{+/+}$ female mouse (top) and age- and sex-matched $p53^{+/m}$ mouse (bottom). Pronounced lordokyphosis, loss of body mass, muscle atrophy and loss of adipose tissue is evident in the $p53^{+/m}$ mouse. **d**–**g**, Comparisons of mean $p53^{+/+}$ (black columns) and $p53^{+/m}$ (white columns) body (**d**), spleen (**e**), liver (**f**) and kidney (**g**) masses. **h**, **i**, Haematoxylin and eosin-stained cross section of 24-month-old $p53^{+/+}$ spleen (**h**) and $p53^{+/m}$ spleen (**i**) at ×10 magnification. White pulp (WP) is indicated by an arrow in the $p53^{+/+}$ spleen. The lack of arteriole-associated white pulp is indicated by an arrow in the $p53^{+/m}$ spleen.

pL53 transgenic mice recapitulated some of the ageing-related phenotypes observed in the $p53^{+/m}$ mice, particularly those related to skin and bone.

Discussion

The $p53^{+/m}$ mice generated in this study were highly resistant to spontaneous tumours. This resistance depends on wild-type p53, as in its absence (for example, the $p53^{-/m}$ mice) the m allele confers little protection from tumours. This is consistent with our hypothesis that the gene product of the m allele augments the activity of wild-type p53 to prevent tumour formation. The tumour resistance of $p53^{+/m}$ mice may be partly intrinsic to the individual cells of the animals, as fibroblasts derived from $p53^{+/m}$ embryos are more resistant to transformation by activated *ras* plus *myc* oncogenes. However, this does not rule out the possibility that systemic changes, such as alterations in hormone or growth factor levels, could contribute to the tumour resistance phenotypes. Despite an enhanced tumour resistance, the $p53^{+/m}$ mice showed a reduced longevity in comparison with their $p53^{+/+}$ littermates. This reduced longevity is associated with the early appearance of a number of ageing-associated phenotypes. These particular ageing phenotypes correlate with a 23% reduction in median lifespan, suggesting that they are important for organismal longevity.

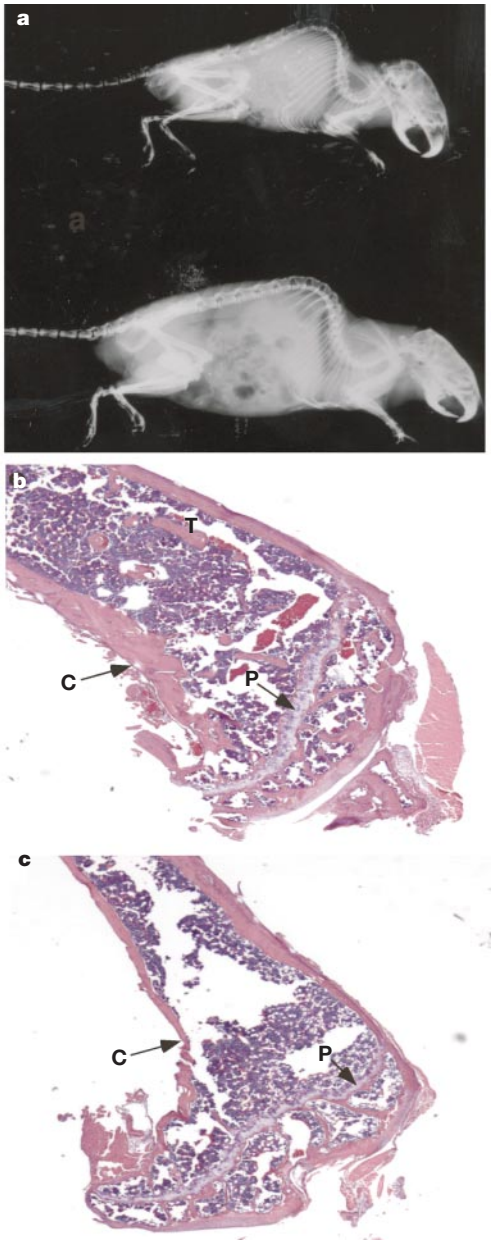

Figure 5 Bone phenotypes in $p53^{+/+}$ and $p53^{+/m}$ mice. **a**, Whole-body radiograph of 24-month-old $p53^{+/m}$ (top) and $p53^{+/+}$ (bottom) mice. **b**, **c**, Haematoxylin and eosin-stained cross-sections of tibias from a 24-month-old $p53^{+/+}$ mouse (**b**) and an age-matched $p53^{+/m}$ mouse (**c**). Note the reduction in cortical bone thickness (C) and absence of trabecular bone (T) in the tibia of the 24-month-old $p53^{+/m}$ mouse (**c**). P, epiphyseal plate.

The extent of the m-allele deletion in the $p53^{+/m}$ mouse has not been completely defined. The p53-associated deletion includes p53 exons 1–6 as well as sequences upstream of the *p53* gene. It is possible that the $p53^{+/m}$-associated phenotypes could be a result of either haploinsufficiency in genes upstream of *p53* or the production of a truncated p53 gene product. Although haploinsufficiency cannot be ruled out, we favour the hypothesis that a truncated C-terminal gene product of p53 is the primary effector (see below). A truncated message capable of expressing the C-terminal p53 protein is expressed in many tissues of the $p53^{+/m}$ mouse, and several laboratories have shown that p53 C-terminal fragments or peptides can augment wild-type p53 activities[35–39]. We have shown that p53 m-allele expression constructs enhance wild-type p53 transactivation activity and can suppress cancer cell growth in the presence of wild-type p53 (S.V., S.D.T., N.G. and H.I., unpublished data). The cells of $p53^{+/m}$ mice have increased wild-type p53 responses to ionizing radiation compared with cells of $p53^{+/-}$ mice. The enhanced tumour resistance in $p53^{+/m}$ mice is dependent on wild-type p53, supporting a model in which the m-allele product requires wild-type p53 to promote tumour suppression. Another p53 mutant line (pL53) recapitulates some early ageing phenotypes of $p53^{+/m}$ mice.

The display of ageing-related phenotypes in the pL53 transgenic mice may seem paradoxical, given that this p53 transgene mutation would be expected to confer a dominant negative activity and inhibit wild-type p53 function. The modest increase in tumour susceptibility indicates that such activity is present. However, because this mutant p53 allele encodes a temperature-sensitive p53 protein, we propose that the pool of transgene-encoded mutant p53 may exist in an equilibrium between wild-type active and mutant inactive conformations. Where body temperatures are presumably lower (near the skin surface), more of the transgene protein may be in a wild-type conformation and thus inhibit proliferation. The reduced adipose tissue, hair growth and wound healing in the older pL53 transgenic animals are consistent with this.

For both $p53^{+/m}$ and pL53 transgenic models, we propose that the early ageing phenotypes are in part a result of enhanced activity of wild-type p53 in some tissues. The reduced cellularity and mass in organs of the older $p53^{+/m}$ mice suggests that organ cell numbers are not maintained. Moreover, some of the ageing phenotypes suggest a reduction in proliferation of stem cells. With the ageing process, this proliferative reserve may decline more rapidly in the $p53^{+/m}$ mice as their stem cells undergo replicative senescence sooner than their $p53^{+/+}$ counterparts. The accumulation of genetic insults in the stem cells of $p53^{+/m}$ mice may provoke enhanced arrest responses that gradually result in fewer division-competent cells. The $p53^{+/m}$ mice eventually reach a point in which the proliferative capacity of stem cells is so reduced that sufficient numbers of mature cells cannot be provided to maintain organ homeostasis. The resulting phenotypes may include reductions in organ mass, function and tolerance for stress.

The data presented here support a role for p53 in the regulation of ageing and longevity in mice. The association of early ageing and tumour resistance in the $p53^{+/m}$ mice is also consistent with the idea that senescence is a mechanism of tumour suppression[4,12,13]. We propose that an ageing-related reduction in stem cell proliferation may have a more important role in longevity than previously recognized. □

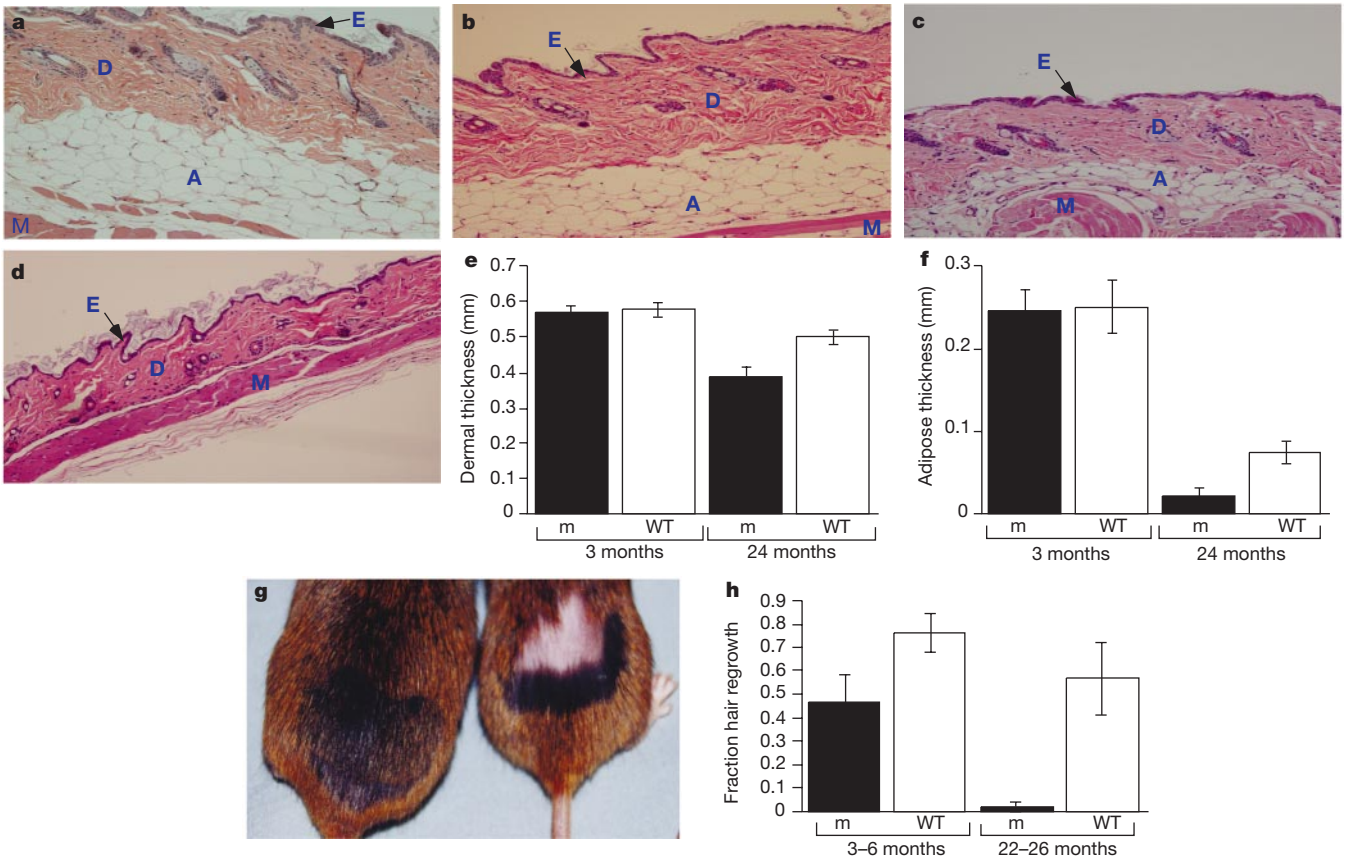

Figure 6 Skin and hair growth phenotypes in $p53^{+/+}$ and $p53^{+/m}$ mice. **a**–**d**, Cross-sections of dorsal skin from a 3-month-old $p53^{+/+}$ mouse (**a**), a 3-month-old $p53^{+/m}$ mouse (**b**), a 24-month-old $p53^{+/+}$ mouse (**c**) and a 24-month-old $p53^{+/m}$ mouse (**d**). Note the reduced thickness of the dermis (D) and subcutaneous adipose tissue (A) in the skin of 24-month-old $p53^{+/m}$ mice (**d**). E, epidermis; M, muscle. Magnification 100×. **e**, **f**, Graphs showing mean dermal thickness (**e**) and mean thickness of subcutaneous adipose layer (**f**) of 3- and 24-month-old $p53^{+/+}$ and $p53^{+/m}$ mice. WT, wild type. **g**, Representative 24-month-old $p53^{+/+}$ mouse (left) and age-matched $p53^{+/m}$ mouse (right) 20 days after removal of hair from a 2-cm^2 dorsal area. **h**, Mean hair growth in 3- and 24-month-old $p53^{+/+}$ and $p53^{+/m}$ mice.

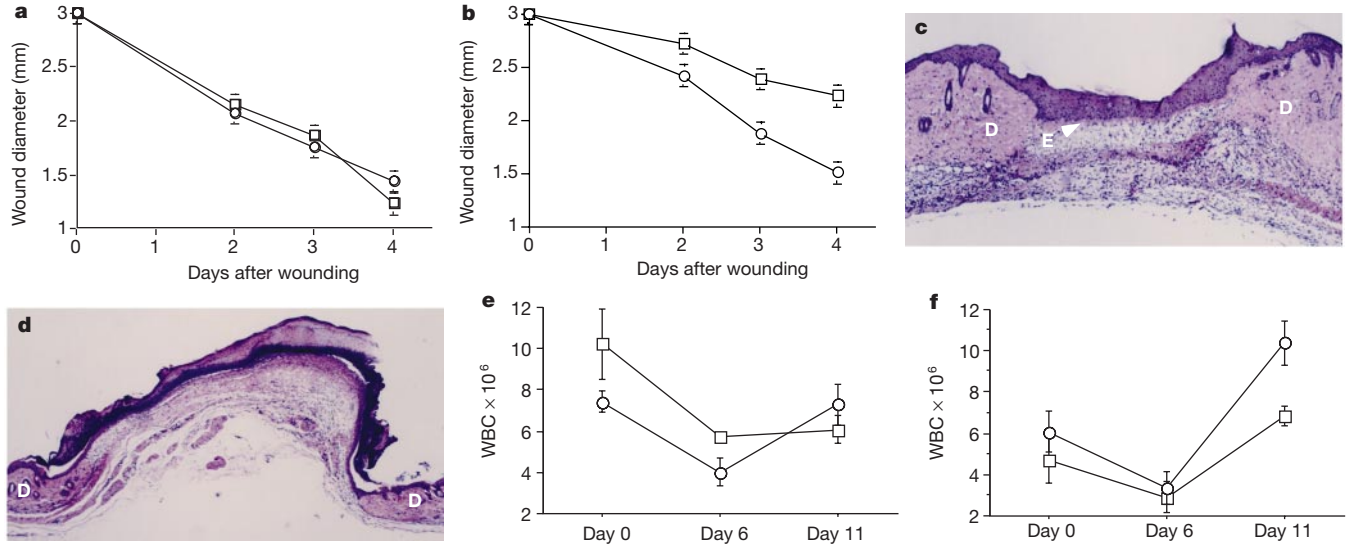

Figure 7 Stress responses in $p53^{+/+}$ and $p53^{+/m}$ mice. **a**, **b**, Graphs showing mean wound diameter in 3- (**a**) and 24-month-old (**b**) $p53^{+/+}$ (circles) and $p53^{+/m}$ (squares) mice at 0, 2, 3 and 4 days after wounding. **c**, **d**, Wound cross-sections stained with haematoxylin and eosin 4 days after wound induction. Representative wounds from 24-month-old $p53^{+/+}$ (**c**) and $p53^{+/m}$ (**d**) mice show reduced re-epithelialization in the $p53^{+/m}$ mice. D, dermis; E, epithelialization. Magnification 100×. **e**, **f**, White blood cell (WBC) counts in 3-month-old (**e**) and 24-month-old (**f**) $p53^{+/+}$ (circles) and $p53^{+/m}$ (squares) mice at 0, 6 and 11 days after 5-FU injection.

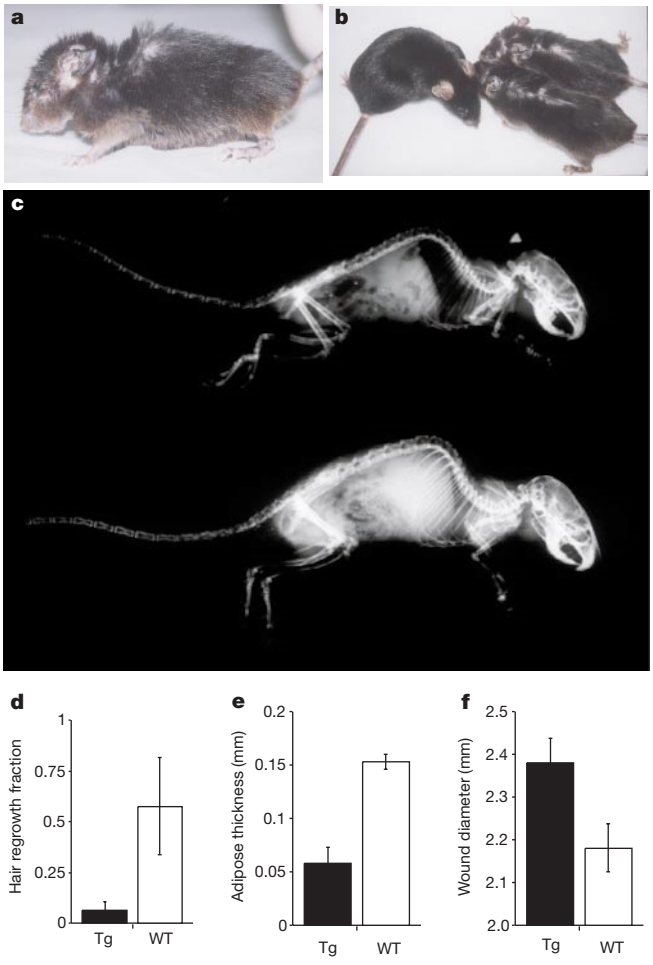

Figure 8 Ageing-related phenotypes observed in pL53 transgenic mice. **a**, Photograph of 20-month-old pL53 transgenic male mouse. **b**, Photograph of two pL53 transgenic (right) and one non-transgenic (left) littermates at 20 months of age. The bedraggled appearance of the transgenic mice was not due to fighting as each of these mice were caged individually. Moreover, all three mice were devoid of tumours. **c**, Radiographs of 18-month-old female pL53 transgenic mouse (top) and non-transgenic mouse (bottom). Note the reduction in bone density in the transgenic female. **d**, Mean hair growth in 16–18-month-old pL53 (Tg) and non-transgenic (WT) mice. **e**, Mean subcutaneous adipose thickness in pL53 transgenic and wild-type 16–18-month-old mice. **f**, Mean wound diameter 4 days after induction by 3-mm biopsy in 16–18-month-old wild-type and pL53 transgenic mice.

Methods

Generation of *p53*$^{+/m}$ mice

The 'hit-and-run' gene targeting approach[40] was used to introduce a mutant p53 targeting construct derived from an exon 2 (*Xho*I) to exon 10 (*Sac*II) genomic clone containing a Arg245Trp point mutation and linked to a PGK promoter-driven hypoxanthine phosphoribosyltransferase (HPRT) selection cassette. Along with the point mutation, we incorporated a *Stu*I site to facilitate subsequent genotyping efforts. One targeted embryonic stem cell clone was isolated that showed incorporation of the point mutation into the endogenous p53 allele but exhibited a deletion of p53 exons 1–6. This clone, containing the p53 mutation designated 'm', was amplified and used to generate chimaeric and germline *p53*$^{+/m}$ mice according to standard methods[41].

Mouse breeding, maintenance and longevity

We generated the mutant p53 m allele in AB1 embryonic stem cells of 129/Sv origin. Chimaeric mice with this mutation were backcrossed two generations into C57BL/6, so that the mice in the *p53*$^{+/m}$ study were mixed inbred C57BL/6–129/Sv mice. *p53*$^{+/m}$ mice of this background were intercrossed with *p53*$^{+/-}$ mice of similar background[19], and the *p53*$^{+/+}$, *p53*$^{+/m}$, *p53*$^{+/-}$ and *p53*$^{-/m}$ offspring were monitored for tumour formation and longevity.

The pL53 transgenic mice[22] were provided by Alan Bernstein in a CD-1 background, and these mice were backcrossed twice into a C57BL/6 background before intercrossing. pL53 transgenic mice were always crossed to *p53*$^{+/+}$ mice of the same background to maintain transgene hemizygosity in the offspring. Littermate mice of different p53 genotypes were usually housed together and fed freely with standard mouse chow over their lifespan. Although the mice were not housed in a pathogen-free environment, morbidity owing to infectious agents was not noted in the colony. Mice exhibiting overt tumours or extreme morbidity were killed and subjected to necropsy.

Mouse genotyping

Two Southern blot assays were necessary to distinguish *p53*$^{+/m}$, *p53*$^{+/+}$, *p53*$^{+/-}$, *p53*$^{-/-}$ and *p53*$^{-/m}$ mice. In the first assay to distinguish the '–' and '+' alleles, tail DNAs were cleaved with *Bam*HI and hybridized to a p53 exon 2–6 cDNA probe as described previously[19]. In the second assay to distinguish the m allele, tail DNAs were cleaved with *Stu*I and hybridized to a p53 exon 5–10 probe. A fragment migrating at 0.9 kb was diagnostic for the m allele. To genotype pL53 transgenic mice, we hybridized tail DNAs cleaved with *Bam*HI with the p53 exon 2–6 cDNA probe. Mice with the mutant p53 transgene exhibit a 10–20-fold increase in hybridization intensity of a 5-kb, p53-specific fragment compared with their non-transgenic counterparts.

RNA analyses

Total RNA was purified from frozen tissue using Trizol Reagent (Gibco BRL) according to the manufacturer's specifications. RT-PCR specific for the m-allele messages and p53 messages was performed on 1 μg total RNA. The m-allele message and p53 message were amplified using PCR primers specific for the leader sequence of the m allele (5′-CGGGCAGGTTCTGAAGGCAGTTTC-3′) and exon 7 of the wild-type p53 allele (5′-TGCATGGGGGGCATGAACCGCCGACC-3′). The downstream primer (5′-CAGCTCCCGGAACATCTCGAA-3′) was anchored in p53 exon 10. 5′ RACE was performed using the Marathon 5′ RACE Kit (Clontech). One microgram of total RNA from spleens of *p53*$^{+/+}$ and *p53*$^{+/m}$ mice was used to distinguish the m-allele message. We gel isolated, cloned and sequenced the differentially migrating band in the *p53*$^{+/m}$ sample. We performed northern and western blot assays as described previously[42].

Transformation and transfection assays

Primary MEFs were plated on 100-mm plates at a density of 10^6 cells per plate in 15% fetal calf serum (FCS) and DMEM growth medium. Cells were treated 24 h after plating with varying titres of a *ras*/*myc* retrovirus diluted in DMEM without FCS for 2 h. After treatment, we added 15% FCS DMEM to the plates. We replaced growth medium every 3 days for 3 weeks. Transformed foci were examined microscopically for transformed cell characteristics before counting. We counted the foci after Giemsa staining. Representative foci of *p53*$^{+/m}$ and *p53*$^{+/+}$ mice were amplified, and 10^6 cells were injected subcutaneously into nude mice. Virtually all foci of both genotypes produced tumours in nude mice. To assay p53 transactivation activity *in vitro*, 60-mm plates of subconfluent Saos-2 cells were transfected with 1 μg of a p21 promoter-luciferase plasmid and 2 μg each of various combinations of cytomegalovirus (CMV) promoter-driven wild-type p53, m allele and empty vector expression plasmids using Lipofectamine Plus reagent (Invitrogen). Cell lysates were prepared 48 h after transfection, and luciferase activity was measured using a Turner TD-20e luminometer and normalized to renilla luciferase according to the instructions provided with the dual-luciferase assay kit (Promega).

Bone analyses

Mice were X-rayed *in situ* under anaesthesia for whole-body X-rays. We used an X-ray dose of 20 kV for 20 s. We prepared and analysed cross-sections of tibias as described previously[43].

Skin, wound healing and hair growth assays

Dorsal skin sections were fixed, embedded in paraffin and stained with haematoxylin and eosin. The thickness of the dermal and adipose layers from the skin samples were determined by taking 10 random measurements along the length of individual skin samples ($n = 4$) for each genotype and age group. Wound healing was assayed as described previously[44], except that full thickness wounds were generated with a 3-mm biopsy punch rather than a 5-mm biopsy punch. For the hair growth assay, age-matched *p53*$^{+/+}$ and *p53*$^{+/m}$ mice (3–6 months and 20–26 months) were shaved on their dorsal surface using an electric razor. We measured hair regrowth 20 days after shaving as described previously[27].

Haematopoietic cell ablation with 5-fluorouracil

Two-month-old and 20-month-old *p53*$^{+/+}$ and *p53*$^{+/m}$ mice were treated with an intraperitoneal bolus injection of 5-FU (100 mg per kg body weight). Peripheral blood was obtained by tail bleeds before injection, and on days 6 and 11 after injection. We analysed peripheral blood counts and haemoglobin amounts by flow cytometry (Technicon Instruments).

Received 29 June; accepted 24 October 2001.

1. Levine, A. J. p53, the cellular gatekeeper for growth and division. *Cell* **88,** 323–331 (1997).
2. Ko, L. J. & Prives, C. p53: puzzle and paradigm. *Genes Dev.* **10,** 1054–1072 (1996).
3. Giaccia, A. J. & Kastan, M. B. The complexity of p53 modulation: emerging patterns from divergent signals. *Genes Dev.* **12,** 2973–2983 (1998).
4. Itahana, K., Dimri, G. & Campisi, J. Regulation of cellular senescence by p53. *Eur. J. Biochem.* **268,** 2784–2791 (2001).

5. Atadja, P., Wong, H., Garkavtsev, I., Geillette, C. & Riabowol, K. Increased activity of p53 in senescing fibroblasts. *Proc. Natl Acad. Sci. USA* **92,** 8348–8352 (1995).
6. Bond, J. A. *et al*. Evidence that transciptional activation by p53 plays a direct role in the induction of cellular senescence. *Oncogene* **13,** 2097–2104 (1996).
7. Webley, K. *et al*. Posttranslational modifications of p53 in replicative senescence overlapping but distinct from those induced by DNA damage. *Mol. Cell. Biol.* **20,** 2803–2808 (2000).
8. Shay, J. W., Pereira-Smith, O. M. & Wright, W. E. A role for both RB and p53 in the regulation of human cellular senescence. *Exp. Cell Res.* **196,** 33–39 (1991).
9. Bond, J. A., Wyllie, F. S. & Wynford-Thomas, D. Escape from senescence in human diploid fibroblasts induced directly by mutant p53. *Oncogene* **9,** 1885–1889 (1994).
10. Gire, V. & Wynford-Thomas, D. Reinitiation of DNA synthesis and cell division in senescent human fibroblasts by microinjection of anti-p53 antibodies. *Mol. Cell. Biol.* **18,** 1611–1621 (1998).
11. Serrano, M., Lin, A. W., McCurrach, M. E., Beach, D. & Lowe, S. W. Oncogenic ras provokes premature cell senescence associated with accumulation of p53 and $p16^{INK4a}$. *Cell* **88,** 593–602 (1997).
12. Sager, R. Senescence as a mode of tumor suppression. *Environ. Health Perspect.* **93,** 59–62 (1991).
13. Campisi, J. Aging and cancer: the double-edged sword of replicative senescence. *J. Am. Geriatric Soc.* **45,** 482–488 (1997).
14. Rudolph, K. L. *et al.* Longevity, stress response, and cancer in aging telomerase-deficient mice. *Cell* **96,** 701–712 (1999).
15. Chin, L. *et al*. p53 deficiency rescues the adverse effects of telomere loss and cooperates with telomere dysfunction to accelerate carcinogenesis. *Cell* **97,** 527–538 (1999).
16. Vogel, H., Lim, D. S., Karsenty, G., Finegold, M. & Hasty, P. Deletion of Ku86 causes early onset of senescence in mice. *Proc. Natl Acad. Sci. USA* **96,** 10770–10775 (1999).
17. Lim, D. S. *et al*. Analysis of ku80-mutant mice and cells with deficient levels of p53. *Mol. Cell. Biol.* **20,** 3772–3780 (2000).
18. Migliaccio, E. *et al.* The $p66^{shc}$ adaptor protein controls oxidative stress response and life span in mammals. *Nature* **402,** 309–313 (1999).
19. Donehower, L. A. *et al.* Mice deficient for p53 are developmentally normal but susceptible to spontaneous tumours. *Nature* **356,** 215–221 (1992).
20. Jacks, T. *et al.* Tumor spectrum analysis in p53-mutant mice. *Curr. Biol.* **4,** 1–7 (1994).
21. Purdie, C. A. *et al*. Tumour incidence, spectrum and ploidy in mice with a large deletion in the p53 gene. *Oncogene* **9,** 603–609 (1994).
22. Lavigueur, A. *et al*. High incidence of lung, bone, and lymphoid tumors in transgenic mice overexpressing mutant alleles of the p53 oncogene. *Mol. Cell. Biol.* **9,** 3982–3991 (1989).
23. Arking, R. *Biology of Aging* 2nd edn 153–250 (Sinauer, Sunderland, Massachusetts, 1998).
24. Kalu, D. N. in *Handbook of Physiology, Section 11: Aging* (ed. Masoro, E. J.) 395–412 (Oxford Univ. Press, New York, 1995).
25. Weiss, A., Arbell, I., Steinhagen Thiessen, E. & Silbermann, M. Structural changes in aging bone: osteopenia in the proximal femurs of female mice. *Bone* **12,** 165–172 (1991).
26. Chuttani, A. & Gilchrest, B. A. in *Handbook of Physiology, Section 11: Aging* (ed. Masoro, E. J.) 309–324 (Oxford Univ. Press, New York, 1995).
27. Harrison, D. E. & Archer, J. R. Biomarkers of aging: tissue markers. Future research needs, strategies, directions and priorities. *Exp. Gerontol.* **23,** 309–321 (1988).
28. Shock, N. W. Aging of physiological systems. *J. Chronic Dis.* **36,** 137–142 (1983).
29. Gerstein, A. D., Phillips, T. J., Rogers, G. S. & Gilchrest, B. A. Wound healing and aging. *Dermatol. Clin.* **11,** 749–757 (1993).
30. Muravchik, S. in *Clinical Anesthesia* 3rd edn (eds Barash, P. G., Cullen, B. F. & Stoelting, R. K.) 1125–1136 (Lippincott-Raven, Philadelphia, 1997).
31. Harvey, R. C. & Paddleford, R. R. Management of geriatric patients. A common occurrence. *Vet. Clin. North Am. Small Anim. Pract.* **29,** 683–699 (1999).
32. Harrison, D. E. Evaluating functional abilities of primitive hematopoietic stem cell populations. *Curr. Top. Microbiol. Immunol.* **177,** 13–30 (1992).
33. Takeda, T. *et al*. Pathobiology of the senescence-accelerated mouse (SAM). *Exp. Gerontol.* **32,** 117–127 (1997).
34. Michalovitz, D., Halevy, O. & Oren, M. Conditional inhibition of transformation and of cell proliferation by a temperature-sensitive mutant of p53. *Cell* **62,** 671–680 (1990).
35. Hupp, T. R., Sparks, A. & Lane, D. P. Small peptides activate the latent sequence-specific DNA binding function of p53. *Cell* **83,** 237–245 (1995).
36. Jayaraman, J. & Prives, C. Activation of p53 sequence-specific DNA binding by short single strands of DNA requires the p53 C-terminus. *Cell* **81,** 1021–1029 (1995).
37. Muller-Tiemann, B. F., Halazonetis, T. D. & Elting, J. J. Identification of an additional negative regulatory region for p53 sequence-specific DNA binding. *Proc. Natl Acad. Sci. USA* **95,** 6079–6084 (1998).
38. Selivanova, G. *et al*. Restoration of the growth suppression function of mutant p53 by a synthetic peptide derived from the p53 C-terminal domain. *Nature Med.* **3,** 632–638 (1997).
39. Selivanova, G., Rybachenko, L, Jannson, E., Iotsova, V. & Wiman, K. G. Reactivation of mutant through interaction of a C-terminal preptide with the core domain. *Mol. Cell. Biol.* **19,** 3395–3402 (1999).
40. Hasty, P., Ramirez-Solis, R., Krumlauf, R. & Bradley, A. Introduction of a subtle mutation into the Hox-2.6 locus in embryonic stem cells. *Nature* **350,** 243–246 (1991).
41. Hogan, B., Beddington, R., Costantini, F. & Lacy, E. *Manipulating the Mouse Embryo: A Laboratory Manual* 2nd edn 189–216 (Cold Spring Harbor Laboratory Press, New York, 1994).
42. Venkatachalam, S. *et al*. Retention of wild-type p53 in tumors from p53 heterozygous mice: reduction of p53 dosage can promote cancer formation. *EMBO J.* **17,** 4657–4667 (1998).
43. Ducy, P. *et al.* Increased bone formation in osteocalcin-deficient mice. *Nature* **382,** 448–452 (1996).
44. Wojcik, S. M., Bundman, D. S. & Roop, D. R. Delayed wound healing in keratin 6a knockout mice. *Mol. Cell. Biol.* **20,** 5248–5255 (2000).

Acknowledgements

We thank X.-J. Wang, G. Van Zant, D. Roop, R. Waikel, P. Biggs, M. Patel, S. Wojcik, R. Levasseur, V. Hortenstine, R. Ford, S. Wojcik, C. Pickering, R. Geske and M. Oren for advice and technical assistance. We also thank G. Lozano for luciferase and p53 plasmids. This study was supported by the National Cancer Institute.

Correspondence and requests for materials should be addressed to L.A.D. (e-mail: larryd@bcm.tmc.edu).